

# An Improved Method and Assessment of Sinusoidal Pulse Width Modulation (SPWM) Inverter for Induction Furnace Operation

Sourav Basu<sup>1</sup>, Sourav Debnath<sup>2\*</sup>, Soumya Mukherjee<sup>3</sup>, Akshay Kumar Pramanick<sup>4</sup>

<sup>1</sup>Department of Electrical Engineering, Camellia School of Engineering & Technology, Kolkata 700124, India

<sup>2</sup>Department of Electrical and Electronics Engineering, Swami Vivekananda Institute of Science and technology, Kolkata - 700145, India. Email: dr.souravdebnath@gmail.com

<sup>3</sup>Department of Metallurgical Engineering, Kazi Nazrul University, Domohani Railway Colony, Kalla More, Asansol 713340, West Bengal, India

<sup>4</sup>Department of Metallurgical & Material Engineering, Jadavpur University, Kolkata 700032, West Bengal, India

\*Corresponding author: Dr. Sourav Debnath, Email: [dr.souravdebnath@gmail.com](mailto:dr.souravdebnath@gmail.com)

**Abstract**—The recent improvements in living standards and economic growth can be partially attributed to the critical role of foundries, which are specialized factories engaged in metal casting. Central to the operation of any foundry is the furnace, whose overall performance and efficiency are significantly influenced by the type of converter used to supply power. Conventional converters, such as resonant converters, often come with complex designs and operational challenges, and they may pose safety risks. In response to these issues, this research focuses on developing a Sinusoidal Pulse Width Modulation (SPWM) inverter to provide a high-quality, pure sinusoidal AC power supply for induction furnaces. The SPWM inverter is favored for this application due to its superior capabilities in output power delivery, energy efficiency, and its ability to minimize harmonic distortion. The main objective of this study is to generate a pure sine wave for the induction furnace, ensuring optimal furnace performance. Initially, the inverter design was developed using Porteous software, followed by its implementation and testing under real-world conditions. The testing results demonstrated that the SPWM inverter consistently produces a pure sine wave across a wide range of frequencies, maintaining low harmonic distortion and achieving outstanding performance.

**Keywords**— Foundry, Induction furnace, SPWM, sine wave, inverter, AC power.

## I. INTRODUCTION

To A foundry is a type of metal casting facility where molten metal is poured into a mold, allowed to cool, and then used to manufacture metal things [1]-[5]. This metal casting process is made feasible by the machinery, tools, protective gear, and other devices found at foundries. But a foundry's main goal is to melt metal, which calls for extreme temperatures. Of course, traditional foundries are inherently hazardous [3]-[6].

For the melting of materials in foundries, furnaces are absolutely necessary. Furnaces should be able to melt materials safely and effectively, generate heat without the need for moisture, and prevent uncontrolled fires. As a result, foundry design addresses the removal of combustible components and the constant availability of fire retardant [8]-[22].

Modern industry's mechanization of foundry operations necessitates the development of new or enhanced materials with stable, high-quality mechanical qualities that are economical and environmentally benign to melt. Reduced manual labor, the employment of relatively less skilled workers, homogeneous mold packing density, fewer casting rejections, faster production rates, and a lower total cost per piece are all benefits of mechanized foundry processes. Today's highly automated foundries use controlled induction furnaces all around the world [7]-[9].

Along with the evolution and diversification of basic foundry operations, furnace technologies have also advanced over time. Overall, rating, furnace operating temperature, automation, and on-site furnace finishing are the most prevalent trends. Compared to earlier generations, modern furnaces are bigger, safer, and more effective. Furnaces are being developed using resonant converters. However, this converter's design and functioning are crucial and contribute to the furnace's bulk [4]-[11].

Induction furnaces are known for their substantial power consumption [1]-[5], which is required for the melting and heating of materials. Despite their high energy demand, these furnaces offer numerous advantages that make them a preferred choice in many industrial applications. Among these benefits are exceptional heating efficiency, a high production rate, and the creation of a cleaner working environment due to the absence of combustion gases and pollutants. The typical setup of an induction furnace includes several key components, namely a rectifier, an inverter, and a heating coil. The rectifier converts the incoming AC power to DC, while the inverter then converts the DC power back into a high-frequency AC current, which is supplied to the heating coil [18]-[20][26]. This process enables precise control over the heating of materials, ensuring both efficiency and safety in the furnace's operation.

The selection of induction furnace coils is primarily based on factors such as the required power capacity, the operating frequency, and the target operating temperature. The coil's ability to generate heat effectively and its overall lifespan are closely tied to the quality of the power supplied to it. Power that is of high quality, specifically characterized by a pure sinusoidal waveform with minimal harmonic distortion, plays a crucial role in optimizing the performance and durability of the heating coil [6]-[12]. By reducing unwanted harmonics and ensuring a smooth, consistent power supply, high-quality power helps to prevent excessive wear and tear on the coil, thereby extending its operational life. This, in turn, leads to improved overall efficiency of the furnace, reducing maintenance costs and enhancing its long-term reliability [8]-[17].

In this study, a pure sine wave inverter has been developed using MOSFET switches along with a three-level Pulse Width Modulation (PWM) technique in an H-bridge configuration. This design effectively manages the MOSFET drivers to control the activation of the MOSFETs within the H-bridge, ensuring smooth and efficient operation. A notable enhancement in this design is the use of a 12V DC supply, which allows for the generation of a clean sine wave output with a stable 50Hz frequency. This frequency can be easily adjusted to meet specific operational requirements. The frequency tuning is achieved by modifying the amplitude of the sine wave reference signal in the control circuit, providing a flexible and precise method to adjust the output frequency as needed for different applications. This approach improves both the efficiency and versatility of the inverter in real-world scenarios.

## II. MOTIVATION OF THE STUDY

### A. Historical Background

After In the eighteenth century, the first model of a furnace was developed, using coal as its primary fuel source to generate heat. While this furnace represented a significant technological advancement at the time, it was plagued by several issues [3]-[8]. The heat distribution within the furnace was uneven, leading to inefficient heating and making it difficult to control the temperature effectively. Furthermore, the use of coal posed serious safety risks, as it contributed to fire hazards and unstable operating conditions. In addition to its operational drawbacks, the furnace had a low overall efficiency, wasting energy and generating a variety of harmful byproducts. Each use of the furnace released pollutants into the environment, including fine dust, toxic gases, and excessive noise. These emissions not only contributed to environmental degradation but also resulted in higher temperatures in the surrounding areas, further exacerbating the furnace's negative impact on both health and the environment [7]-[24].

With the continuous progress of technology and ongoing research throughout the nineteenth century, the development of electricity-operated furnaces emerged as a significant advancement in industrial heating [9]-[20]. These electric furnaces offered notable improvements over their coal-powered predecessors, providing enhanced safety and higher operational efficiency. The use of electricity reduced many of the risks associated with combustible fuels, such as fire hazards and toxic emissions, while also offering more precise temperature control. However, despite these advantages, the electric furnace came with its own set of challenges. One of the primary drawbacks was the limited ability to control the current, which can impact the furnace's performance under certain conditions. Additionally, electricity-operated furnaces tend to consume more power compared to earlier models, resulting in higher energy costs [2]-[10]. Furthermore, these furnaces often require a larger physical footprint, which demands more space and land, making them less suited for facilities with limited available area. These factors, while improving upon older designs, still presented challenges for widespread adoption in some industrial settings.

The modern mechanized foundry requires a furnace that is not only energy-efficient and environmentally friendly but also offers precise control and ensures safe, quiet operation [15]-[22]. To meet these demanding requirements, the integration of advanced power electronic converters is essential. When the power supplied to the furnace's heating unit is in the form of a pure sinusoidal waveform, the furnace operates more smoothly, which in turn leads to significant improvements in both efficiency and overall performance. A smooth, sinusoidal power supply minimizes distortions and reduces stress on the furnace components, thereby extending their lifespan and optimizing energy usage. The primary aim of this study is to design and develop an advanced inverter capable of providing a pure sinusoidal output to the furnace unit. This innovation is expected to enhance the furnace's operational efficiency, reduce energy consumption, and improve both the reliability and sustainability of the foundry's operations [10]-[13].

## III. METHODOLOGY AND MODELING

The block diagram of the induction furnace is presented in Fig. 1. In this study, significant efforts have been focused on developing a compact and modular Sinusoidal Pulse Width Modulation (SPWM) inverter. This innovative design offers a high degree of flexibility, allowing it to be easily scaled to accommodate different power requirements. By adjusting the ratings of the inverter, it can be seamlessly integrated with an induction furnace to meet specific operational needs. This scalability feature makes the inverter adaptable to a wide range of furnace sizes and power capacities, enhancing its versatility and ensuring it can be customized for various industrial applications. As a result, this modular approach provides a practical and cost-effective solution for optimizing furnace performance across different operational conditions.

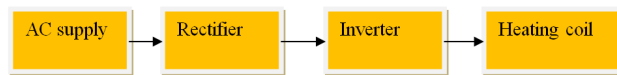


Fig. 1 Schematic representation of an induction furnace system

When building the heating unit of an induction furnace, two types of heating materials are typically preferred: silicon carbide-based heating elements and molybdenum-based heating elements [2]–[15]. Molybdenum is utilized to create temperatures of around 2,000°C, whereas silicon carbide may achieve temperatures as high as 1,750°C [2]–[19].

*A. Implementation of SPWM inverter*

At the outset, the sine wave signal is routed to a non-inverting amplifier, where it undergoes amplification while preserving its original phase. Subsequently, the amplified sine wave signal and the triangular wave signal are directed to a summing junction. At this point, the two signals are combined to form a composite waveform. This resulting output from the summing junction, along with the amplified sine wave signal, is then forwarded to the input of a comparator, where further signal processing takes place.

In this configuration, the high-side output of the comparator is directly connected to the high-side input of the first MOSFET driver, ensuring proper signal transmission to control the high-side operation of the first driver. Similarly, the low-side output of the comparator is linked to the low-side input of the first MOSFET driver, enabling control of its low-side operation. Furthermore, the high-side output of the first MOSFET driver is interconnected with the low-side input of the second MOSFET driver, while the low-side output of the first MOSFET driver is connected to the high-side input of the second MOSFET driver. This interlinking establishes a complementary relationship between the two MOSFET drivers, facilitating efficient operation and signal coordination across the system.

An H-bridge is strategically placed between the two MOSFET drivers, serving as a critical component for enabling signal switching and polarity reversal. This configuration ensures precise control of the output waveform necessary for efficient operation. Following the H-bridge, a low-pass LC filter is implemented to remove high-frequency components and smooth out the signal, ensuring that only the desired frequency range is transmitted. The resulting filtered signal is then directed to the furnace coils, where it generates the required electromagnetic field for the heating process in the induction furnace. This arrangement optimizes the signal quality and ensures the reliable performance of the system.

*B. Implementation process*

A 12V power supply is essential for generating both the sine wave and the carrier wave, providing the necessary energy for the waveform generators to function. The waveform generators operated reliably, allowing both waveforms to be produced simultaneously without interference. Significant effort during the thesis was devoted to fine-tuning these waveforms, ensuring that the frequency, shape, and amplitude of the resulting PWM signal met the required specifications. This refinement process was crucial for achieving precise and stable signal characteristics. However, certain challenges arose during this phase, which impacted the development process. These challenges, along with their implications, are outlined in detail in the limitations section below.

All functional blocks in the system were successfully implemented, ensuring the generation of a stable PWM signal. The sine wave signal was first passed through an amplifier to achieve the required amplitude, after which it, along with the carrier wave signal, was routed to the designated comparator. The comparator processed these inputs and forwarded the resulting signal to the H-Bridge drivers, where the PWM signal was applied to control the switching mechanism.

To achieve this, H-Bridge driver chips were assembled on a breadboard. Each driver chip was equipped with four N-channel MOSFETs, enabling efficient signal modulation and switching. In the final stage of the project, a carefully designed low-pass filter was integrated across the load connected to the H-Bridge. This filter played a crucial role in smoothing the output, eliminating high-frequency noise, and delivering the desired waveform to the connected system. The design and implementation of these components adhered to references [4], [20]–[24], ensuring theoretical and practical alignment throughout the process.

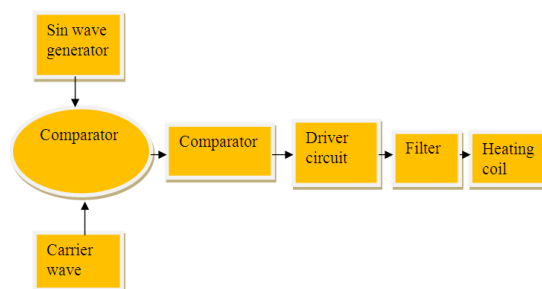


Fig. 2 Development methodology for the SPWM inverter

C. Sine Wave Generator

To generate a sine wave output, a Bubba oscillator was selected due to its robust design and reliable performance. The circuit diagram illustrating this configuration is provided in the figure above. The LM348 operational amplifier was employed in the oscillator circuit, chosen for its affordability and suitability for this application.

The Bubba oscillator is structured into four distinct stages, each capable of providing an output signal. These outputs are accessible at points labeled P2 through P5 within the circuit. Among these points, P2 generates the highest amplitude output, but it also introduces the most significant distortion into the signal. On the other hand, P5 produces an output with the smallest amplitude, but this is accompanied by the least distortion, making it ideal for applications requiring high signal purity. Given this trade-off, P5 was selected as the optimal point for signal extraction to ensure the least distorted sine wave output for further processing.

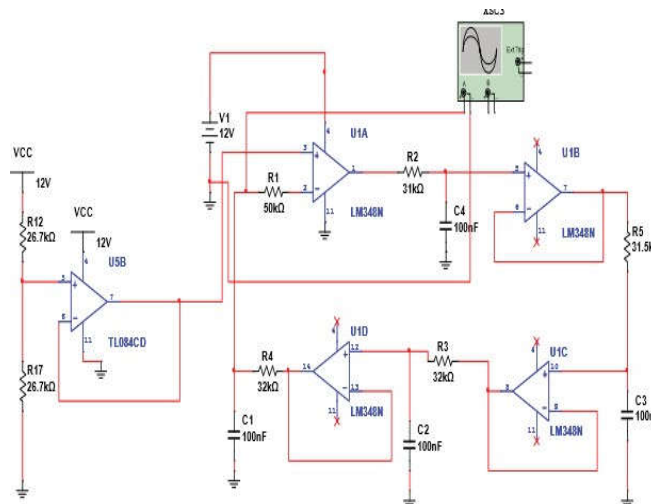


Fig. 3 Sinewave generator

D. Carrier Wave Generator

The carrier wave used in pulse width modulation (PWM) applications can typically take the form of either a triangular or sawtooth waveform. For this design, a triangular wave was chosen as the carrier signal due to its favorable characteristics for achieving precise modulation. The frequency of the triangular wave was set to 1 kHz, a value determined through simulations that optimized for minimal peak power loss, ensuring efficient system performance.

The generation of the triangular wave was accomplished using analog circuitry. This process involved employing an integrator circuit, which produces the triangular waveform by integrating a square wave input over time. This method is both straightforward and reliable, making it a practical choice for generating the required carrier signal. The use of analog components also provides a high level of control and stability in maintaining the waveform's desired frequency and amplitude.

For generating the triangular wave, the TL-084 operational amplifier was selected due to its reliable performance in waveform generation tasks. The operational amplifier was biased with a voltage of 12V, as specified in the circuit design, to ensure optimal operation within the required parameters. This specific configuration of the TL-084 amplifier, combined with the appropriate biasing, enables the generation of a stable and consistent triangular wave, making it highly suitable for the intended application. The stability of the waveform is crucial for ensuring accurate modulation and efficient signal processing in the overall system, meeting the performance requirements of the project. References [21]-[24] provide further details on the design considerations and the successful implementation of this approach.

E. PWM-Pulse Width Modulation

In this study, a three-level Pulse Width Modulation (PWM) technique is utilized to analyze the interaction between the reference sine wave and the triangular wave. By employing this advanced modulation method, the technique allows for a more accurate and detailed comparison of the two waveforms, enhancing the precision of the modulation process. The three-level PWM approach introduces additional control over the switching points, resulting in a finer resolution and more effective modulation of the signal. This improved modulation scheme contributes to enhanced performance, reducing harmonic distortion and improving the efficiency of the generated output, thus ensuring better overall system behavior.

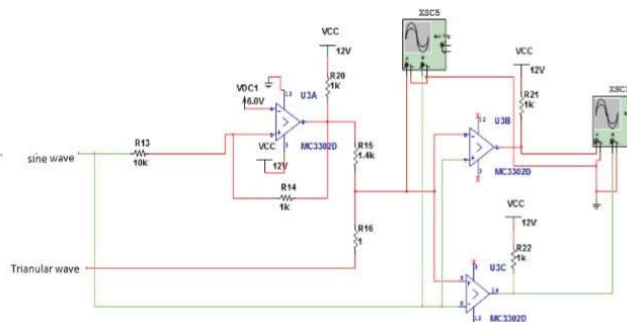


Fig. 5 PWM implementation

F. H-Bridge MOSFET

The H-Bridge is an essential electronic circuit designed to control the direction of the voltage applied to a load, allowing for bidirectional current flow. It consists of four switches arranged in a specific configuration, which enables precise control over the voltage polarity applied across the load. When Switches 1 and 4 are closed while Switches 2 and 3 remain open, a positive voltage is applied to the load, resulting in forward current flow. Conversely, when Switches 2 and 3 are closed, while Switches 1 and 4 are open, a reverse voltage is applied, causing current to flow in the opposite direction.

It is vital to carefully manage the switching operation to avoid any short circuits. Specifically, all four switches should never be closed at the same time, as this would create a direct short across the power supply, potentially damaging the components and causing system failure. Proper control logic is required to ensure that these conditions are avoided, maintaining safe and efficient operation of the H-Bridge.

To reduce power loss and enhance switching speed, N-channel MOSFETs were selected for this design, as they offer superior efficiency compared to other transistor types. N-channel MOSFETs are particularly effective in switching applications due to their low on-resistance and high current-carrying capacity, which minimizes power dissipation during operation. To drive the high-side MOSFETs in the H-Bridge, MOSFET drivers were incorporated into the circuit. Specifically, the IR2110 N-channel MOSFET driver was chosen for its reliable performance and seamless compatibility with the circuit's needs. The IR2110 is well-suited for driving high-side N-channel MOSFETs, offering features such as high-voltage tolerance and efficient gate-drive capability. This choice ensures effective switching of the H-Bridge, contributing to improved overall system performance by providing fast, reliable, and efficient operation under varying load conditions. References [16]-[21] detail the performance characteristics and advantages of using the IR2110 in this particular application.

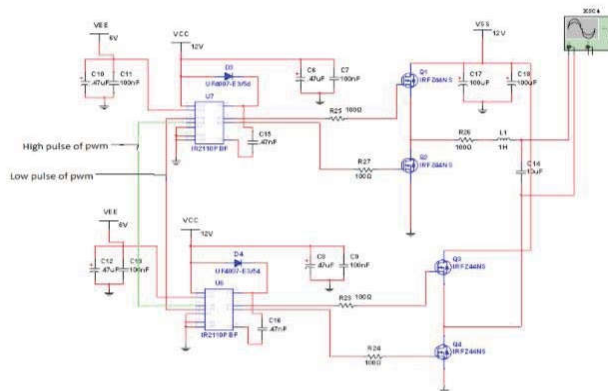


Fig. 6 H-bridge Driver with Filter Circuit

G. Circuit on the Printed Circuit Board (PCB)

After successfully completing the simulation and testing of all individual components, the next step involved implementing the design onto a Printed Circuit Board (PCB). To create the PCB layout, the Proteus software was employed, which provided a comprehensive platform for designing and organizing the circuit components on the board. The software allowed for precise placement and routing of components, ensuring optimal signal flow and minimizing potential issues such as noise or interference. This stage was essential for translating the theoretical design into a physical, functional circuit. The layout process was carefully carried out to ensure that the final PCB would meet the performance and reliability requirements for practical applications. Proper PCB design is critical, as it directly impacts the stability, manufacturability, and long-term durability of the circuit once deployed in real-world systems.

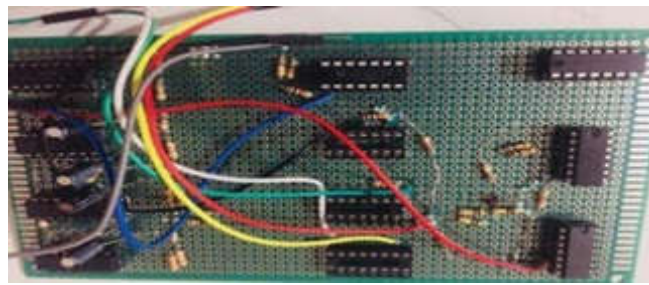


Fig. 7 Circuit on PCB

#### IV. RESULT ANALYSIS

For this research, a 12-volt DC input was chosen to generate a 50 Hz AC output. Before proceeding with the physical implementation, extensive simulations were conducted using Proteus software. The simulations were carefully examined to assess the accuracy, reliability, and overall performance of the design. This step was crucial, as it allowed for an in-depth evaluation of the circuit's behavior under various conditions, ensuring that the theoretical design would function as intended in practice. By thoroughly analyzing the simulation results, we were able to identify potential issues, make necessary adjustments, and fine-tune the parameters to optimize the system. This rigorous simulation process played a key role in validating the design and ensuring that the final implementation would meet the required specifications.

##### A. Sine Wave Output

The simulated output voltage of the sine wave was measured at 3.5 volts peak-to-peak with a frequency of 50 Hz, which was the intended operating condition. Initially, when the oscillator was first assembled, the output was recorded at 6 volts peak-to-peak, which was higher than expected. After thoroughly reviewing and recalculating all parameters, as well as selecting more suitable components, the team addressed several issues that were causing the circuit to malfunction. These issues were primarily related to improper component selection and incorrect configuration. Once these adjustments were made, and the amplification value was increased, the circuit started to oscillate as intended. Upon visually inspecting the output, the waveform resembled a smooth, stable 50 Hz sine wave, confirming that the oscillator was now functioning correctly and generating the desired output with the correct characteristics.

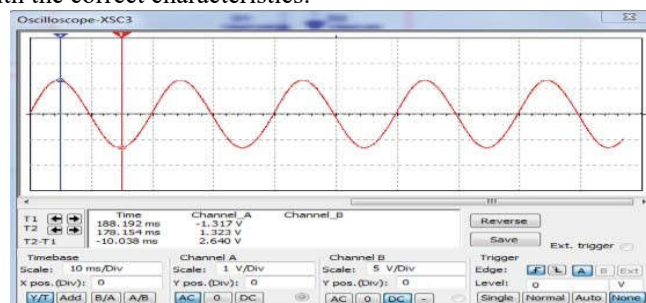


Fig. 8 Simulated sine wave output

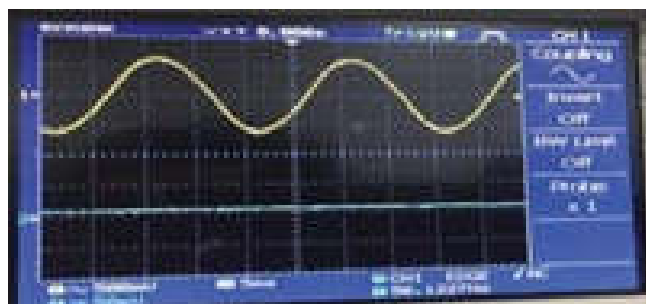


Fig. 9 Original sine wave output



Fig. 10 Amplified signal output

*B. Carrier wave generator*

To generate the carrier wave, a triangular wave was employed due to its desirable properties for modulation purposes. The triangular wave produced a peak-to-peak output voltage of 6 volts and operated at a frequency of 1.02 kHz. This specific waveform was selected because its linear rise and fall provide a stable and consistent basis for generating the carrier signal. The triangular wave's characteristics, including its amplitude and frequency, are crucial for ensuring efficient modulation within the system. By using this waveform as the foundation, the system can effectively modulate the output signal, achieving the desired performance and ensuring reliable operation in the overall system design.

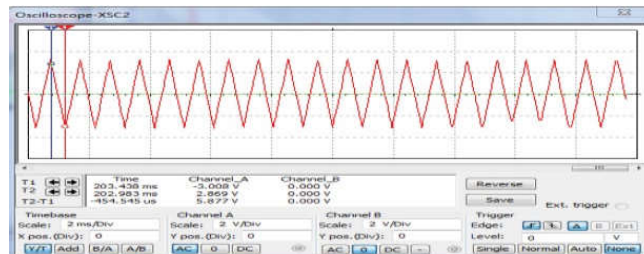


Fig. 11 Simulated carrier wave output

The TL-084 operational amplifier was used to generate the carrier wave, with a 12V non-inverting reference applied to ensure proper operation. To convert the square wave into a triangular wave, resistors R8 (10 kΩ) and R9 (400 kΩ) were placed between operational amplifier stages U4A and U4B. Additionally, two diodes were incorporated to regulate the direction of current flow, ensuring the correct waveform polarity. Initially, the output did not meet the expected specifications. After troubleshooting, we identified the issue and resolved it by replacing resistor R10 with a 5 kΩ resistor, instead of the original 1 kΩ, and by changing the capacitor C5 from 1 μF to 100 pF. These adjustments allowed us to fine-tune the circuit, resulting in the successful completion of the carrier wave section. This process ensured that the carrier wave met the required characteristics, enabling its effective use in the overall system for this research.



Fig. 12 Actual output of the carrier signal

*C. Amplified sine and triangular waves*

Upon amplifying the signal, obtained a peak-to-peak output of 3.48 volts for the sine wave and 6.2 volts for the carrier wave. The respective frequencies for these outputs were measured at 50 Hz for the sine wave and 1.02 kHz for the carrier wave. These results indicate successful amplification and generation of the desired waveforms.

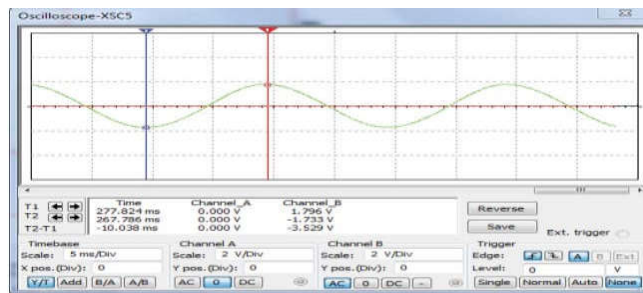


Fig. 13 Amplified sine waveform

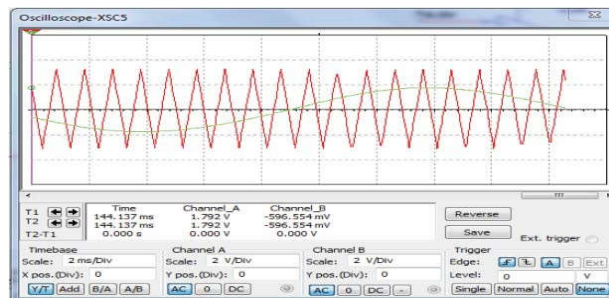


Fig. 14 Comparison of sine wave and triangular wave

## V. CONCLUSION

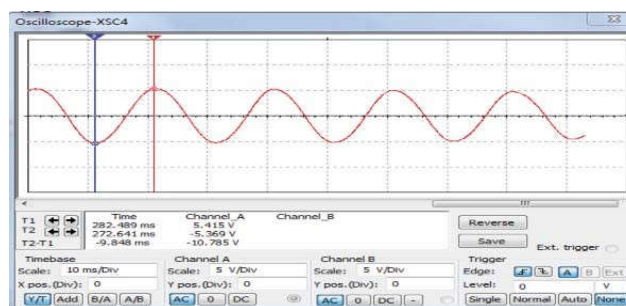


Fig. 15 Pure sinusoidal output

The control signals within the circuit were managed with great precision, ensuring the accurate switching of the H-Bridge MOSFETs. This careful control resulted in the generation of a 50 Hz sine waveform, as illustrated in Fig. 15. The output was successfully produced using a 12V input voltage and a 300-ohm load, after the construction and integration of the LC filter. Despite the proper functioning of the circuit, the resulting output waveform exhibited a peak-to-peak amplitude of only 10 volts. This discrepancy can be attributed to the low ratio between the sine wave and the triangular wave control signals, which limited the overall amplitude of the output. The low amplitude emphasizes the importance of optimizing the control signal ratios to achieve higher output voltages and more efficient signal modulation in future implementations.

If gain of the reference non-inverting sine amplifier is increased, comparatively higher output can be achieved. This adjustment allows the amplifier to produce a peak-to-peak output of 320 volts when the input voltage to the H-Bridge is set at 170V. The increased amplification ensures that the system can handle the higher voltage requirements while maintaining signal integrity. Additionally, by fine-tuning the resistor values in the Bubba oscillator circuit—used to generate the sine wave—the frequency of the output signal can be precisely adjusted. This level of control over both the amplitude and frequency of the signal is crucial for optimizing the performance of the system, allowing it to meet the specific requirements of high-voltage operation. Induction furnaces with nichrome or silicon carbide heating coils are capable of making temperature up to 500°C. These furnaces are being used for heat treatment of non-ferrous alloys, tempering ferrous alloys, for stress relief after welding and shaping, moreover fabrication of composites.

## REFERENCES

- [1] M.A.Ghalib, Y.S.Abdalla, R.M.Mostafa, "Design and Implementation of a Pure Sine Wave Single Phase Inverter for Photovoltaic Applications," Zone 1 Conference of the American Society for Engineering Education, pp. 1-8, April, 2014, U.S.A.
- [2] R. S. Parmar and S. V. Arya, "Triggering circuit of induction furnace with power quality analysis," 2016 International Conference on Electrical, Electronics, and Optimization Techniques (ICEEOT), Chennai, India, 2016, pp. 3922-3926, doi: 10.1109/ICEEOT.2016.7755450.



- [3] A. C. Moreira, L. C. P. da Silva and H. K. M. Paredes, "Electrical modelling and power quality analysis of three-phase induction furnace," *2014 16th International Conference on Harmonics and Quality of Power (ICHQP)*, Bucharest, Romania, 2014, pp. 415-419, doi: [10.1109/ICHQP.2014.6842822](https://doi.org/10.1109/ICHQP.2014.6842822).
- [4] Vivek R. Gandhewar, Satish V. Bansod, Atul B. Borade (2011). "Induction Furnace- A Review," *International Journal of Engineering and Technology*, vol. 3 (4), pp. 277-284.
- [5] E. Kardas (2012) "Evaluation of Efficiency of Working Time of Equip ment in Blast Furnace Department," *Journal of Achievements in Materials and Manufacturing Engineering*, vol. 55, issue 2, pp. 876-880.
- [6] Digvijay D. Patil, Dayanand A. Ghatge (2017). "Parametric Evaluation of Melting Practice on Induction Furnace to improve Efficiency and System Productivity of CI and SGI Foundry-A Review", *International Advanced Research Journal in Science, Engineering and Technology*, vol. 4, special issue-1, pp. 159-163. DOI [10.17148/IARJSET/NCDMETE.2017.36](https://doi.org/10.17148/IARJSET/NCDMETE.2017.36)
- [7] Uma Kulkarni, Sushant Jadhav, Mahantesh Magadam (2014). "Design and Control of Medium Frequency Induction Furnace for Silicon Melting," *International Journal of Engineering Science and Innovative Technology (IJESIT)*, Volume 3, Issue 4, July 2014.
- [8] Hou, Y. J., Tian, H. M., Qu, X. D., Teng, J. Z., Liu, G. X. and Yan Li (2018). "Development of digital control system for medium frequency induction furnaces," *IOP Conf. Series: Earth and Environmental Science* 188 (2018) 012005, doi:[10.1088/1755-1315/188/1/012005](https://doi.org/10.1088/1755-1315/188/1/012005)
- [9] Sanjay R Joshi, Viralkumar Solanki: "Simulation of Induction Furnace And Comparison With Actual Induction Furnace", *International Journal of Recent Technology and Engineering (IJRTE)*, Volume-2, Issue-4, pp. 105-109, September 2013.
- [10] S. Dieckerhoff, M. J. Ruan and R. W. De Doncker, "Design of an IGBT-based LCL-resonant inverter for high-frequency induction heating," *Conference Record of the 1999 IEEE Industry Applications Conference. Thirty-Forth IAS Annual Meeting (Cat. No. 99CH36370)*, Phoenix, AZ, USA, 1999, pp. 2039-2045 vol.3, doi: [10.1109/IAS.1999.806017](https://doi.org/10.1109/IAS.1999.806017).
- [11] Borislav Dimitrov, Khaled Hayatleh, Steve Barker, Gordana Collier, "Design, Analysis and Experimental Verification of the Self-Resonant Inverter for Induction Heating Crucible Melting Furnace Based on IGBTs Connected in Parallel," *Electricity* 2021, 2(4), 439-458; <https://doi.org/10.3390/electricity2040026>
- [12] Ilker Yilmaz, Muammer Ermis, Isik Cadirci, "Medium-Frequency Induction Melting Furnace as a Load on the Power System," *IEEE Xplore*, 48(4):1 – 12, 2011. DOI:[10.1109/IAS.2011.6074408](https://doi.org/10.1109/IAS.2011.6074408)
- [13] Khan, J. Tapson and I De Vries, "Automatic Frequency Control of an Induction Furnace", *Proc. IEEE Coil, Africon '99*, vol.2, September 1999. DOI:[10.1109/IAS.2011.6074408](https://doi.org/10.1109/IAS.2011.6074408)
- [14] Jim Doucet Dan Eggleston Jeremy ShawMQP Terms ABC2006- 2007. Available: [https://web.wpi.edu/Pubs/E-project/Available/E-project-042507-092653/unrestricted/MQP\\_D\\_1\\_2.pdf](https://web.wpi.edu/Pubs/E-project/Available/E-project-042507-092653/unrestricted/MQP_D_1_2.pdf)
- [15] Linda Hassaine, Abdelhamid Mraoui "Control Strategy based on SPWM Switching Patterns for Grid Connected Photovoltaic Inverter", *AIP Conference Proceedings*, 1814(1):020031, 2017. DOI:[10.1063/1.4976250](https://doi.org/10.1063/1.4976250)
- [16] M. B. Cheema, S. A. Hasnain, M. M. Ahsan, M. Umer and G. Ahmad, "Comparative analysis of SPWM and square wave output filtration based pure sine wave inverters," *2015 IEEE 15th International Conference on Environment and Electrical Engineering (EEEIC)*, Rome, Italy, 2015, pp. 38-42, doi: [10.1109/EEEIC.2015.7165289](https://doi.org/10.1109/EEEIC.2015.7165289).
- [17] Texas Instruments "800VA Pure Sine Wave Inverter's Reference Design", Application Report, SLAA602A–June 2013–Revised August 2017. Available: <https://www.ti.com/lit/an/slaa602a/slaa602a.pdf>
- [18] Vikas VitthalRokade, Sandip Subhash Bangale, Vinod Sambhaji Gaikwad & Aslam Usman Mujawar," Simple 100 watt inverter," *Shri Vitthal Education & Research Institute, Pandharpur*, January 2002. Availble: [sverian.sveri.ac.in/downloads/cod/EE/EE.46-49.pdf](http://sverian.sveri.ac.in/downloads/cod/EE/EE.46-49.pdf)
- [19] Abdelsalam Shaaban, Jean Thomas, Ramadan Mahmoud Mostafa, "Design and Implementation of a Single Phase Sinusoidal Pulse Width Modulation Inverter Based Microcontroller for Wind Energy Conversion Systems," *Research Journal of Applied Sciences, Engineering and Technology* 14(2):86-94, February 2017. DOI:[10.19026/rjaset.14.3994](https://doi.org/10.19026/rjaset.14.3994)
- [20] Sohaib Aslam, Sundas Hannan, Arsalan Haider, and Mohammad Hamza Tariq, "Exploring PIC 24F series Microcontroller using MPLAB and Proteus" , *JOURNAL OF CURRENT RESEARCH IN SCIENCE*, vol. 4, No. 2, 2016.
- [21] P. Panagis, F. Stergiopoulos, P. Marabeas and S. Manias, "Comparison of state of the art multilevel inverters," *2008 IEEE Power Electronics Specialists Conference*, Rhodes, Greece, 2008, pp. 4296-4301, doi: [10.1109/PESC.2008.4592633](https://doi.org/10.1109/PESC.2008.4592633).
- [22] M. Malinowski, K. Gopakumar, J. Rodriguez and M. A. Pérez, "A Survey on Cascaded Multilevel Inverters," in *IEEE Transactions on Industrial Electronics*, vol. 57, no. 7, pp. 2197-2206, July 2010, doi: [10.1109/TIE.2009.2030767](https://doi.org/10.1109/TIE.2009.2030767).
- [23] E. Samadaei, A. Sheikholeslami, S. A. Gholamian, and J. Adabi, "A Square T-Type (ST-Type) Module for Asymmetrical Multilevel Inverters," *IEEE Transactions on Power Electronics*, vol. 33, no. 2, pp. 987–996, 2018. DOI:10.1109/TPEL.2017.2675381
- [24] S. P. Gautam, L. Kumar, and S. Gupta, "Single-phase multilevel inverter topologies with self-voltage balancing capabilities," *IET Power Electronics*, vol. 11, no. 5, pp. 844–855, 2018.
- [25] B. Mahato, S. Mittal, S. Majumdar, K. C. Jana, and P. K. Nayak, "Multilevel Inverter with Optimal Reduction of Power Semi-conductor Switches," in *Renewable Energy and its Innovative Technologies*, Springer Singapore, 2019, pp. 31–50.
- [26] Sheikh Tanzim Meraj, Nor Zaihar Yahaya, Kamrul Hasan, Molla Shahadat Hossain Lipu, Ammar Masaoud, Sawal Hamid Md Ali, Aini Hussain, Muhammad Murtadha Othman and Farhan Mumtaz "Three-Phase Six-Level Multilevel Voltage Source Inverter: Modeling and Experimental Validation," *Micromachines* 2021, 12(9), 1133, pp. 1-16, 2021. <https://doi.org/10.3390/mi12091133>